

Øyvind Nordbø · John Wyller · Gaute T. Einevoll

# Neural network firing-rate models on integral form

## Effects of temporal coupling kernels on equilibrium-state stability

Received: date / Accepted: date

**Abstract** Firing-rate models describing neural network activity can be formulated in terms of differential equations for the synaptic drive from neurons. Such models are typically derived from more general models based on Volterra integral equations assuming exponentially decaying temporal coupling kernels describing the coupling of pre- and postsynaptic activities. Here we study models with other choices of temporal coupling kernels. In particular, we investigate the stability properties of constant solutions of two-population Volterra models by studying the equilibrium solutions of the corresponding autonomous dynamical systems, derived using the linear chain trick, by means of the Routh-Hurwitz criterion. In the four investigated synaptic-drive models with identical equilibrium points we find that the choice of temporal coupling kernels significantly affects the equilibrium-point stability properties. A model with an  $\alpha$ -function replacing the standard exponentially decaying function in the inhibitory coupling kernel is in most of our examples

found to be most prone to instability, while the opposite situation with an  $\alpha$ -function describing the excitatory kernel is found to be least prone instability. The standard model with exponentially decaying coupling kernels is typically found to be an intermediate case. We further find that stability is promoted by increasing the weight of self-inhibition or shortening the time constant of the inhibition.

**Keywords** neural networks · firing rate · Volterra · stability · temporal coupling · Routh-Hurwitz

---

Ø. Nordbø  
Department of Mathematical Sciences and Technology and  
Center for Integrative Genetics, Norwegian University of Life  
Sciences, P.O.Box 5003, 1432 Ås, Norway  
Tel.: +47-73593955  
Fax: +47-73592889  
E-mail: oyvind.nordbo@sintef.no  
*Present address:* SINTEF Energy Research, 7465 Trondheim,  
Norway

J. Wyller  
Department of Mathematical Sciences and Technology and  
Center for Integrative Genetics, Norwegian University of Life  
Sciences, P.O.Box 5003, 1432 Ås, Norway  
Tel.: +47-64965489  
Fax: +47-64965401  
E-mail: john.wyller@umb.no

G.T. Einevoll  
Department of Mathematical Sciences and Technology and  
Center for Integrative Genetics, Norwegian University of Life  
Sciences, P.O.Box 5003, 1432 Ås, Norway  
Tel.: +47-64965433  
Fax: +47-64965401  
E-mail: gaute.einevoll@umb.no

---

## 1 Introduction

Following pioneering work of, e.g., Wilson and Cowan (1973) and Amari (1977) in the 1970's, a tradition has developed for studying simplified cortical-network models using field descriptions. In this approach the individual times for firing of action-potentials are not modeled, only the firing rate, that is, the probability densities for firing. Likewise, a continuum description of the set of neurons constituting the neural network is typically used so that the neural firing activities can be described by scalar fields in terms of a time and one or two space coordinates. Neural field models have been widely used to investigate generic features such as the generation and/or stability of coherent structures such as spatially localized bumps, spatially or spatiotemporally oscillating patterns, and travelling waves, pulses and fronts. For reviews of the comprehensive literature, see Ermentrout (1998), Bressloff (2005), Coombes (2005) and Vogels et al. (2005).

Existing firing-rate models are typically formulated in terms of sets of ordinary differential equations. For *synaptic-drive* models (Pinto et al. 1996; Ermentrout 1998) each ordinary differential equation has the form

$$\tau_j \frac{du_j}{dt} + u_j = g_j \left( \sum_k w_{jk} u_k \right) \quad (1)$$

where a physiological interpretation is that  $u_j$  is the 'synaptic drive' from neural element  $j$  (Pinto et al. 1996),  $\tau_j$  is a time constant reflecting the decay of this synaptic drive following an action-potential in element  $j$ , and  $w_{jk}$  is the synaptic weight from element  $k$  onto element  $j$ .  $g_j(x)$  is the firing-rate function of neural element  $j$ , converting the net synaptic drive onto element  $j$  into a firing rate. This function is typically assumed to have a sigmoidal form.

The firing-rate model in (1) can be derived from Volterra integral-equation models with exponentially decaying temporal coupling kernels (Ermentrout 1998; Dayan and Abbott 2001). The dynamics described by (1) corresponds to

$$u_j(t) = h_j(t) * g_j\left(\sum_k w_{jk} u_k(t)\right), \quad \text{where} \quad (2)$$

$$h_j(t) = \frac{1}{\tau_j} e^{-t/\tau_j} \quad (3)$$

and the 'asterisk' denotes a temporal convolution.

The form of (2) clarifies the above physiological interpretation of the temporal coupling kernel  $h_j(t)$ : it describes the temporal form of the 'synaptic drive'  $u_j$  following firing of an action potential in element  $j$  as felt in the soma of its postsynaptic neurons. This temporal form will reflect the temporal form of the synaptic current (i.e., the type of postsynaptic receptors), the distance from the synapse to the soma of the postsynaptic neuron, as well as electrical properties of the postsynaptic dendrites. While the assumption of an exponentially decaying temporal kernel may be reasonable in some situations, it is also clear that this cannot generally be the case. For example, a synaptic input current with an exponentially decaying temporal shape onto a distal part of an apical dendrite of a large layer-5 pyramidal neuron, will not result in an instantaneous and exponentially decaying disturbance of the somatic potential: while the disturbance will be initiated immediately, the maximum disturbance will come some time later. Even a synaptic input at a fast AMPA synapse at the basal dendrites appears to give an EPSP at the soma that resembles an  $\alpha$ -function more than a decaying exponential (see Fig. 18.1 in Koch (1999)).

In the present study we investigate stability properties of equilibrium states in firing-rate models of the type in (2) with various types of temporal coupling kernels  $h_j(t)$ . This issue of the properties of the background state is getting more important as one starts to explore network models where the dynamics is determined by a combination of the background state and stimulus-evoked input (Vogels et al. 2005). The common choice of studying rate models of the type in (1), mainly motivated by mathematical convenience, implicitly corresponds to assuming exponentially decaying temporal kernels (3). Here we consider two-population models (excitatory+inhibitory) and, in particular, investigate the consequences of choosing other temporal kernels than

the exponential kernel, i.e.,  $\alpha$ -functions ( $\sim t \exp(-t/\tau)$ ,  $t > 0$ ) which has its maximum at time  $t = \tau$ . This function is commonly used to model synaptic currents and conductances, see, e.g., Ch. 5 in Dayan and Abbott (2001).  $\alpha$ -function temporal coupling kernels have also been used in previous investigations of stability properties of such background states in other neural network models (Hutt et al. 2003; Hutt and Atay 2005; Atay and Hutt 2006).

In the analysis we employ the 'linear chain trick' (Cushing 1977), previously used in a neural network context by, e.g., Laing and Longtin (2003), to reformulate the Volterra systems as sets of coupled differential equations which are then analyzed by means of dynamical systems theory. In particular, we investigate the stability of the equilibrium point by means of the Routh-Hurwitz criterion and use Hopf's theorem to investigate the existence of generic Hopf bifurcations as stability is lost (Ermentrout and Cowan 1979a).

## 2 Generalization of firing-rate model

We consider a two-population (excitatory+inhibitory) synaptic-drive model where the starting point is the following Volterra equation system,

$$u_e = h_e * g_e(w_{ee}u_e - w_{ei}u_i) \quad (4)$$

$$u_i = h_i * g_i(w_{ie}u_e - w_{ii}u_i) \quad (5)$$

where  $u_e$  ( $u_i$ ) denote the excitatory (inhibitory) 'synaptic drive'.  $g_n$  is the firing-rate function modelled by means of a piecewise linear function (Tsodyks et al. 1997; Koch 1999; Tatenò et al. 2004),

$$g_n(x_n) = \begin{cases} 0, & x_n < \theta_n \\ \beta_n(x_n - \theta_n), & \theta_n \leq x_n \leq \theta_n + 1/\beta_n \\ 1, & x_n \geq \theta_n + 1/\beta_n \end{cases} \quad (n = e, i) \quad (6)$$

The time history of the network is given by the convolution integral  $h_n * g_n$ , ( $n = e, i$ ) defined as

$$(h_n * g_n(x_n))(t) \equiv \int_{-\infty}^t h_n(t-s)g_n(x_n(s))ds \quad (7)$$

The non-negative parameters  $w_{mn}$ ,  $m, n = e, i$ , represent the synaptic weights, and  $\theta_n$ ,  $n = e, i$ , is the activity threshold for firing for the excitatory and inhibitory populations.  $\beta_n$  measures the steepness of the firing-rate function. Finally, the temporal kernels  $h_n$  are normalized, i.e.,  $\int_0^\infty h_n(t)dt = 1$ , continuous and bounded.

First, notice that the following properties hold true independent of the specific choice of temporal kernels:

- Since  $g_n$ ,  $n = e, i$ , is Lipschitz continuous and bounded and the  $h$ -kernels are continuous and bounded, we know, according to Appendix A, that the system will be globally well-posed.

- The scaling transformation

$$w_{mn} = \beta_m^{-1} \tilde{w}_{mn}, \quad \theta_n = \beta_n^{-1} \tilde{\theta}_n \quad (8)$$

shows that we may put the scaling parameter to  $\beta_n = 1$  without loss of generality. In what follows we assume  $\beta_n = 1$  and drop the tilde notation.

- The constant solutions of (4)-(5) are independent of the temporal kernels  $h$ . For the oblique part of the firing-rate function, i.e., when  $\theta_n < x_n < \theta_n + 1$ , the coordinates of these solutions  $(u_e, u_i) \equiv (u_e^{(0)}, u_i^{(0)})$  are given as (Tsodyks et al. 1997)

$$u_e^{(0)} = \frac{w_{ei}\theta_i - (1 + w_{ii})\theta_e}{w_{ei}w_{ie} + (1 - w_{ee})(1 + w_{ii})} \quad (9)$$

$$u_i^{(0)} = \frac{(w_{ee} - 1)\theta_i - w_{ie}\theta_e}{w_{ei}w_{ie} + (1 - w_{ee})(1 + w_{ii})} \quad (10)$$

Moreover since  $0 \leq g_n(x) \leq 1$ , it follows from the system (4)-(5) that  $0 \leq u_n \leq 1$  (where  $n = e, i$ ). From the expressions (9)-(10) we see that the latter condition imposes the conditions (i)  $\text{sgn}[N] = \text{sgn}[D]$ , and (ii)  $|D| > |N|$ , where  $D$  and  $N$  denote the denominator and numerator.

In what follows we will investigate the equilibrium states, i.e., the constant solutions, and their stability properties for the model (4)-(5) using the standard exponentially decaying coupling kernels as well as three model variations with different choices of temporal coupling kernels for the excitatory ( $h_e(t)$ ) and inhibitory populations ( $h_i(t)$ ). To be specific, we consider

$$\text{Standard: } h_e(t) = e^{-t}, \quad h_i(t) = \frac{1}{\tau} e^{-t/\tau} \quad (11)$$

$$\text{Model A: } h_e(t) = e^{-t}, \quad h_i(t) = \frac{t}{\tau^2} e^{-t/\tau} \quad (12)$$

$$\text{Model B: } h_e(t) = t e^{-t}, \quad h_i(t) = \frac{1}{\tau} e^{-t/\tau} \quad (13)$$

$$\text{Model C: } h_e(t) = t e^{-t}, \quad h_i(t) = \frac{t}{\tau^2} e^{-t/\tau} \quad (14)$$

for  $t \geq 0$ . All kernels are causal, i.e.,  $h(t < 0) = 0$ . Note that the time constant of the excitatory coupling kernel in all cases is set to unity (without loss of generality), and the inhibitory kernel time constant  $\tau$  is thus measured in units of this excitatory kernel time constant. In Fig. 1 we illustrate the forms of the two types of temporal kernels considered: the exponentially decaying kernel ( $\sim \exp(-t/\tau)$ ) and the  $\alpha$ -function kernel ( $\sim t \exp(-t/\tau)$ ).

By using the linear chain trick (Cushing 1977) as described in detail in Appendix A, we derive autonomous dynamical systems governing the time evolution of smooth solutions of the system (4)-(5) for the four choices of temporal kernels listed above. The constant solutions (9)-(10) can be expressed in terms of the equilibrium points of the corresponding dynamical systems. Thus the stability properties of the constant solutions of (4)-(5) can be translated into stability properties of the corresponding equilibrium points. It should be noted that

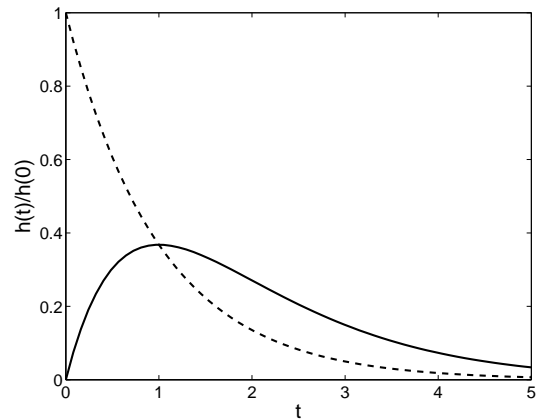


**Fig. 1** Illustration of temporal kernels considered. Solid line: exponentially decaying ( $h(t) = \exp(-t/\tau)H(t)/\tau$ ;  $H(t)$  is Heaviside unit step function.). Dashed line:  $\alpha$ -function ( $h(t) = t \exp(-t/\tau)H(t)/\tau^2$ ).  $\tau = 1$ .

the stability properties of the equilibrium points in general turn out to be determined by only four parameters:  $\tau$ ,  $w_{ee}$ ,  $w_{ii}$ , and the product  $w_{ei}w_{ie}$ . Here we will consider two special situations with a restricted parameter space in detail: (i) All synaptic weights are equal ( $w = w_{ee} = w_{ei} = w_{ie} = w_{ii}$ ), i.e., two freely varying parameters  $\tau$  and  $w$ . (ii) Self-excitation is equal to one ( $w_{ee} = 1$ ), i.e., three freely varying parameters  $\tau$ ,  $w_{ii}$ , and  $w_{ei}w_{ie}$ .

## 2.1 Standard temporal coupling kernel

We first review the properties of the standard two-population firing-rate model corresponding to the temporal kernels in (11). With our choice of a piecewise linear firing-rate function (6) this corresponds to the system studied by Tsodyks et al. (1997). The Volterra equation system (4)-(5) can in this case be converted to a 2D autonomous dynamical system by means of the linear chain trick (Cushing 1977):

$$u_e' = -u_e + g_e(w_{ee}u_e - w_{ei}u_i) \quad (15)$$

$$\tau u_i' = -u_i + g_i(w_{ie}u_e - w_{ii}u_i) \quad (16)$$

As noted above,  $\tau$  is the ratio between the inhibitory and the excitatory timescales. Since the firing-rate function is a piecewise linear function, the system (15)-(16) is a linear system on each of the linear segments. Let us consider the part of this system for which  $0 < u_n < 1$ ,  $n = e, i$ . The Jacobian of the RHS of (15)-(16) is in this case given as

$$\mathbf{J}_s = \begin{bmatrix} w_{ee} - 1 & -w_{ei} \\ w_{ie}/\tau & -(1 + w_{ii})/\tau \end{bmatrix} \quad (17)$$

Since the system (15)-(16) is a 2D system, the stability issue of the equilibrium points given by (9) and (10) can

be completely resolved by means of the invariants of the Jacobian, i.e., by means of the trace and the determinant:

$$\text{tr}[\mathbf{J}_s] = w_{ee} - 1 - (1 + w_{ii})/\tau \quad (18)$$

$$\det[\mathbf{J}_s] = (1 + w_{ii} - w_{ee} + w_{ei}w_{ie} - w_{ee}w_{ii})/\tau \quad (19)$$

from which it follows that stability is obtained provided

$$w_{ee} - 1 - (1 + w_{ii})/\tau < 0, \quad \text{and} \quad (20)$$

$$1 + w_{ii} - w_{ee} + w_{ei}w_{ie} - w_{ee}w_{ii} > 0 \quad (21)$$

In the complementary regime the equilibrium is unstable.

Now, let us consider our two special cases: (i) when  $w = w_{ee} = w_{ei} = w_{ie} = w_{ii}$  we get stability for  $0 < \tau \leq 1$ ,  $w > 0$  and  $\tau > 1$ ,  $w < w_{sH}(\tau)$  where

$$w_{sH}(\tau) = (\tau + 1)/(\tau - 1) \quad (22)$$

Moreover, the theory elaborated in Appendix B shows that the curve  $\tau > 1$ ,  $w = w_{sH}(\tau)$  represents a Hopf bifurcation. It should be noted that Hopf's theorem also applies in the present situation despite the choice of a piecewise linear firing-rate function (6). This theorem presupposes that the vector field defining the dynamical system is at least three times continuously differentiable in an open simple connected subset about the equilibrium point (Perko 2000). This means that in the present situation where the equilibrium points occur at the oblique part of the firing-rate functions, Hopf's theorem is applicable.

(ii) When  $w_{ee} = 1$ , we have  $\text{tr}[\mathbf{J}_s] < 0$  and  $\det[\mathbf{J}_s] > 0$  for the whole parameter space from which it follows we always have stability.

## 2.2 Model A

The first variation we consider to the standard model is a model where the exponentially decaying temporal kernel of the inhibitory population  $h_i(t)$  is replaced by an  $\alpha$ -function (12). As shown in Appendix A, for this model the linear chain trick produces the following 3D autonomous system,

$$u'_e = -u_e + g_e(w_{ee}u_e - w_{ei}u_i) \quad (23)$$

$$\tau u'_i = -u_i + y_i \quad (24)$$

$$\tau y'_i = -y_i + g_i(w_{ie}u_e - w_{ii}u_i) \quad (25)$$

for the time evolution of the synaptic drives. Here  $y_i$  is an auxiliary variable defined as

$$y_i(t) = \frac{1}{\tau} \int_{-\infty}^t e^{-(t-s)/\tau} g_i(w_{ie}u_e(s) - w_{ii}u_i(s)) ds \quad (26)$$

The Jacobian  $\mathbf{J}$  of the system (23)-(25) evaluated at the equilibrium point of this system is given as

$$\mathbf{J} = \begin{bmatrix} w_{ee} - 1 & -w_{ei} & 0 \\ 0 & -1/\tau & 1/\tau \\ w_{ie}/\tau & -w_{ii}/\tau & -1/\tau \end{bmatrix} \quad (27)$$

The characteristic equation  $P_3(\lambda)$  of this matrix is given as

$$P_3(\lambda) = \lambda^3 + a_1\lambda^2 + a_2\lambda + a_3 \quad (28)$$

where the coefficients are given by:

$$a_1 = 2/\tau - w_{ee} + 1 \quad (29)$$

$$a_2 = (2\tau - 2w_{ee}\tau + w_{ii} + 1)/\tau^2 \quad (30)$$

$$a_3 = (1 - w_{ii}w_{ee} + (w_{ii} - w_{ee}) + w_{ei}w_{ie})/\tau^2 \quad (31)$$

The Routh-Hurwitz criterion presented in Appendix B is now used to determine the stability properties. For our first special case,  $w = w_{ee} = w_{ei} = w_{ie} = w_{ii}$ , we find after some algebra that the region in parameter space predicting stable equilibria will be bounded from above by  $w_{AH}(\tau)$ , where

$$w_{AH}(\tau) = \frac{2(\tau + 1)^2}{2\tau^2 + 2\tau - 1 + \sqrt{2\tau^3 - 2\tau + 1}} \quad (32)$$

We now use the synaptic weight as a control parameter and investigate the transversality conditions by means of the theory worked out in Appendix B.2. We find that two eigenvalues cross the imaginary eigenvalue axis transversally when  $w = w_{AH}(\tau)$ , and that the remaining eigenvalue is nonzero. Hence we can conclude that the threshold function  $w_{AH}(\tau)$  represents a generic Hopf bifurcation in this model.

For our second special case,  $w_{ee} = 1$ , we find that the equilibrium is stable if and only if  $\eta < \eta_{AH}(\tau, w_{ii})$ , where  $\eta$  is given as the product of the cross-connection synaptic weights ( $\eta = w_{ei}w_{ie}$ ), and

$$\eta_{AH}(\tau, w_{ii}) = 2(1 + w_{ii})/\tau \quad (33)$$

We now use  $\eta$  as control parameter and find that the curve  $\eta_{AH}(\tau, w_{ii})$  corresponds to a transversal crossing of the imaginary eigenvalue axis, and that the remaining eigenvalue is nonzero. Hence we can conclude that the threshold value  $\eta_{AH}(\tau, w_{ii})$  also corresponds to a generic Hopf bifurcation.

## 2.3 Model B

We now investigate the analogous model where the  $\alpha$ -function integral kernel is assumed for the excitatory population while the inhibitory kernel is modelled as a decaying exponential (13). The corresponding dynamic system can be obtained directly from the model-A equation set in (23)-(25) by the transformation

$$u_e \longrightarrow u_i, \quad u_i \longrightarrow u_e, \quad y_i \longrightarrow y_e, \quad \theta_e \longrightarrow \theta_i, \quad \theta_i \longrightarrow \theta_e \quad (34)$$

and the parameter transformation

$$\begin{aligned} w_{ee} &\longrightarrow -w_{ii}, & -w_{ei} &\longrightarrow w_{ie} \\ w_{ie} &\longrightarrow -w_{ei}, & -w_{ii} &\longrightarrow w_{ee}, & \tau^{-1} &\longrightarrow \tau \end{aligned} \quad (35)$$

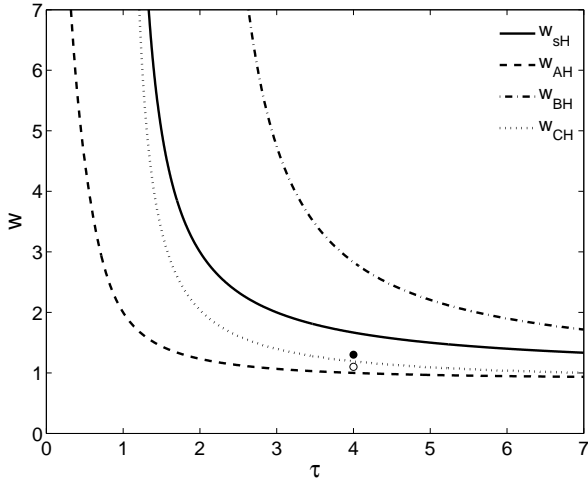


**Fig. 2** Curves separating parameter regimes predicting stable (below curves) and unstable equilibria (above curves) for our four models when synaptic weights are equal, i.e.,  $w = w_{ee} = w_{ei} = w_{ie} = w_{ii}$ . Solid line: standard model,  $w_{sH}(\tau)$  (22). Dashed line: model A,  $w_{AH}(\tau)$  (32). Dash-dotted line: model B,  $w_{BH}(\tau)$  (36). Dotted line: model C,  $w_{CH}(\tau)$  (50). The open dot corresponds to the point  $\tau = 4, w = 1.1$  while solid dot corresponds to the point  $\tau = 4, w = 1.3$ , cf. Fig. 3.

in the Jacobian (27). Again, we appeal to the Routh-Hurwitz criterion in order to resolve the stability issue: For the special case  $w = w_{ee} = w_{ei} = w_{ie} = w_{ii}$ , we find that when  $0 < \tau \leq 2$  the equilibrium is stable for all  $w$ . When  $\tau > 2$  we find that the region in the parameter space predicting stable equilibria will be bounded from above by  $w_{BH}(\tau)$ , where

$$w_{BH}(\tau) = \frac{-\tau^2 + 2\tau + 2 + \tau^2 \sqrt{1 - 2/\tau + 2/\tau^3}}{\tau - 2} \quad (36)$$

We again make use of  $w$  as control parameter and find that two eigenvalues cross the imaginary eigenvalue axis when  $w = w_{BH}(\tau)$ . Further, the remaining eigenvalue is nonzero, and the separatrix defined by (36) is again found to correspond to a generic Hopf bifurcation.

Next, let us consider the special case when the synaptic weight of the self-excitation is put equal to one. Using the cross-connection parameter as control parameter ( $\eta = w_{ei}w_{ie}$ ), we find that the equilibrium in this case is stable if and only if  $\eta < \eta_{BH}(\tau, w_{ii})$ ,

$$\eta_{BH}(\tau, w_{ii}) = 4(w_{ii} + 1) + 2(1 + w_{ii})^2/\tau \quad (37)$$

The Hopf bifurcation conditions in Appendix B.2 are fulfilled, and we can hence conclude that (37) corresponds to a generic Hopf bifurcation.

#### 2.4 Model C

In the last model considered both temporal kernels are modelled as  $\alpha$ -functions (14). In this case the linear chain

trick converts the Volterra system to the 4D autonomous dynamical system

$$u'_e = -u_e + y_e \quad (38)$$

$$\tau u'_i = -u_i + y_i \quad (39)$$

$$y'_e = -y_e + g_e(w_{ee}u_e - w_{ei}u_i) \quad (40)$$

$$\tau y'_i = -y_i + g_i(w_{ie}u_e - w_{ii}u_i) \quad (41)$$

where the pair of auxiliary variables  $(y_e, y_i)$  are defined as

$$y_e(t) = \int_{-\infty}^t e^{-(t-s)} g_e(w_{ee}u_e(s) - w_{ei}u_i(s)) ds \quad (42)$$

$$y_i(t) = \frac{1}{\tau} \int_{-\infty}^t e^{-(t-s)/\tau} g_i(w_{ie}u_e(s) - w_{ii}u_i(s)) ds \quad (43)$$

The Jacobian  $\mathbf{J}$  of the system (38)-(41) evaluated at the equilibrium point (9,10) is now given as

$$\mathbf{J} = \begin{bmatrix} -1 & 0 & 1 & 0 \\ 0 & -1/\tau & 0 & 1/\tau \\ w_{ee} & -w_{ei} & -1 & 0 \\ w_{ie}/\tau & -w_{ii}/\tau & 0 & -1/\tau \end{bmatrix} \quad (44)$$

The characteristic equation  $P_4(\lambda)$  of this coefficient matrix is given as

$$P_4(\lambda) = \lambda^4 + a_1\lambda^3 + a_2\lambda^2 + a_3\lambda + a_4 \quad (45)$$

where the coefficients are given by

$$a_1 = 2(1 + 1/\tau) \quad (46)$$

$$a_2 = (-w_{ee}\tau^2 + 4\tau + w_{ii} + \tau^2 + 1)/\tau^2 \quad (47)$$

$$a_3 = (2\tau - 2w_{ee}\tau + 2w_{ii} + 2)/\tau^2 \quad (48)$$

$$a_4 = (1 - w_{ii}w_{ee} + (w_{ii} - w_{ee}) + w_{ei}w_{ie})/\tau^2 \quad (49)$$

For the special case  $w = w_{ee} = w_{ei} = w_{ie} = w_{ii}$ , we now find from the Routh-Hurwitz criterion that the equilibrium is stable for all  $w$  when  $0 < \tau \leq 1$ . For  $\tau > 1$  the equilibrium is stable when  $w < w_{CH}(\tau)$  where  $w_{CH}(\tau)$  is given as

$$w_{CH}(\tau) = \frac{(\tau + 1)^2(\tau + 1 - \sqrt{\tau})}{\tau^3 - 1} \quad (50)$$

The Hopf bifurcation conditions in Appendix B.2 are fulfilled, and hence we can conclude that (50) corresponds to a generic Hopf bifurcation.

For the special case  $w_{ee} = 1$  the Routh-Hurwitz criterion implies that the system is stable when the cross-connection synaptic weight  $\eta = w_{ei}w_{ie}$  is less than a threshold value  $\eta_{CH}(\tau, w_{ii})$  where

$$\eta_{CH}(\tau, w_{ii}) = \frac{(w_{ii} + 1)(4\tau^2 + 4\tau + w_{ii} + 1)}{\tau(\tau + 1)^2} \quad (51)$$

Again the Hopf bifurcation conditions in Appendix B.2 are fulfilled, and hence we conclude that (51) also corresponds to a generic Hopf bifurcation.

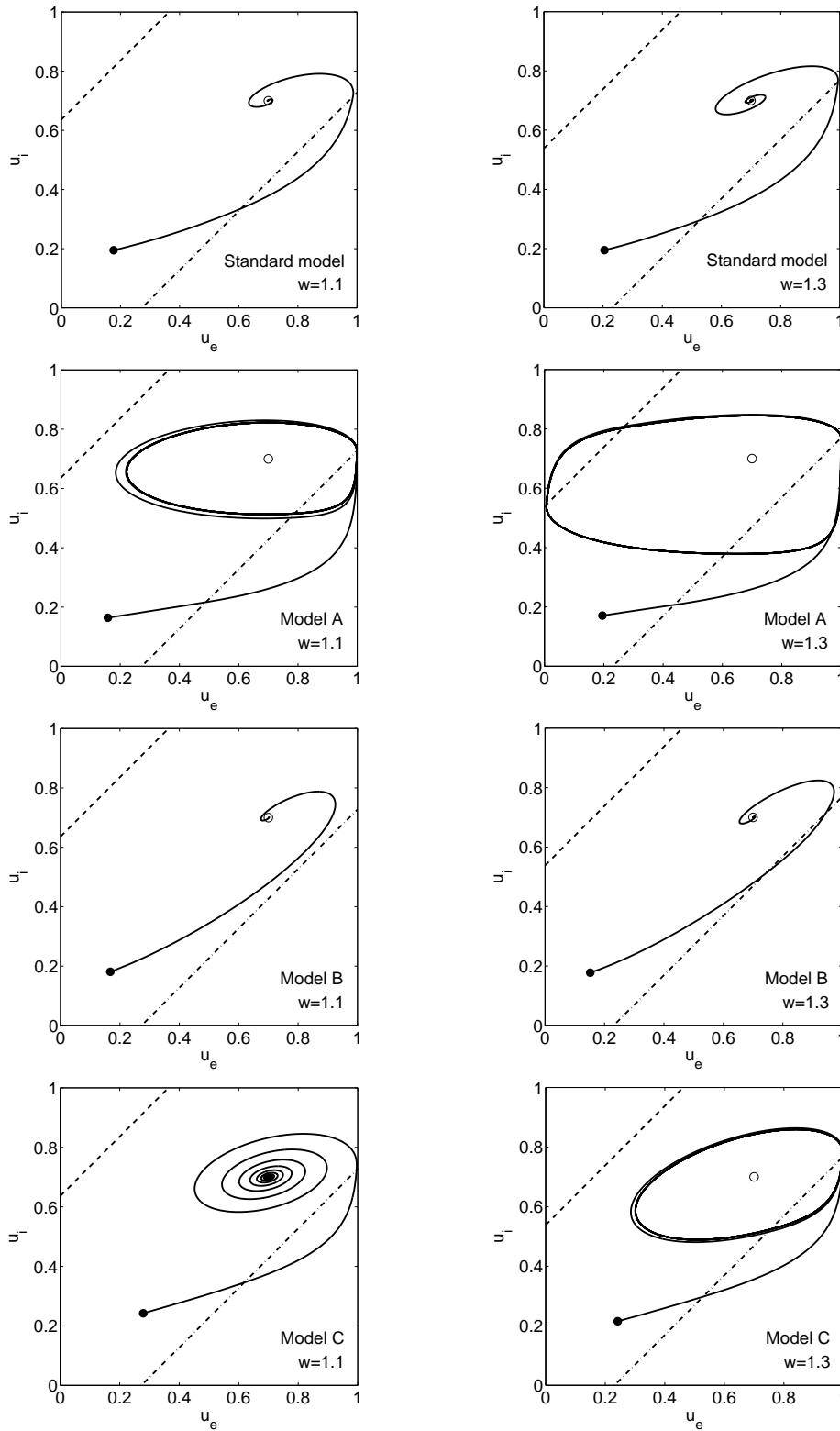


**Fig. 3** Numerical examples of dynamical evolution of the different models for situation with identical synaptic weights,  $w_{ee} = w_{ei} = w_{ie} = w_{ii} = w$ ,  $\theta_e = \theta_i = \theta = -0.7$ , and  $\tau = 4$ . Left column corresponds to  $w = 1.1$ , i.e., open dot in Figure 2, while right column corresponds to  $w = 1.3$ , i.e., solid dot in Figure 2. The equations governing the dynamics are: (15,16) for the standard model, (23-25) for model A, (23-25) with the transformations (34,35) for model B, and (38-41) for model C. The solid dots correspond to initial values of  $(u_e, u_i)$  in the numerical simulations while the open dots correspond to the equilibrium points. Dashed line corresponds to  $w(u_e - u_i) = \theta$  and dot-dashed line to  $w(u_e - u_i) = \theta + 1$ , and the region between these lines thus corresponds to network activity on the oblique part of the firing-rate function, cf. (4)-(6) (with  $\beta_e = \beta_i = 1$ ).

## 2.5 Comparison of model results

We now compare the results regarding stability of the equilibrium in the four models considered for our two special cases: (i) equal synaptic weights and (ii) self-excitation set to unity. Note that the equilibrium points are the same for all models and are given by (9,10).

*All synaptic weights equal.* When all synaptic weights are equal, i.e.,  $w = w_{ee} = w_{ei} = w_{ie} = w_{ii} > 0$ , stability of the equilibrium points is assured in the standard model (11) for  $\tau \leq 1$  or when  $w < w_{sH}(\tau)$  for  $\tau > 1$ , see (22). For the other models the stability of the common equilibrium point (9,10) is as follows: In model A (12) one has stability for all  $\tau$  when  $w < w_{AH}(\tau)$ , see (32). In model B (13) stability is assured for  $\tau \leq 2$  and for  $w < w_{BH}(\tau)$  for  $\tau > 2$ , see (36). In model C (14) one has stability for all  $\tau \leq 1$  and for  $w < w_{CH}(\tau)$  for  $\tau > 1$ , see (50). The parameter regimes predicting stable and unstable equilibria are shown in Figure 2.

From (22),(32), and (50) it follows that the inequalities

$$w_{AH}(\tau) < w_{CH}(\tau) < w_{sH}(\tau) \quad (52)$$

are fulfilled for all  $\tau > 1$ . For  $\tau \leq 1$  model C and the standard model is always stable. Thus we can conclude that for all  $\tau > 0$  the stable regime of model A is contained within the stable regime of model C, which again is contained within the stable regime of the standard model, cf. Figure 2. Further, from (36) and (22) it follows that

$$w_{sH}(\tau) < w_{BH}(\tau) \quad (53)$$

for all  $\tau > 2$ . For  $\tau \leq 2$  model B is always stable, so we can further conclude that the stable regime of the standard model is contained in the stable regime of model B for all  $\tau > 0$ , cf. Figure 2.

To illustrate the parameter-dependence of the stability issue, we show in Figure 3 examples of dynamical evolution for the four models considered for two particular parameter sets,  $w = 1.1, \tau = 4$  and  $w = 1.1, \tau = 4$ , cf. Figure 2. These points are chosen so that they are immediately below and above, respectively, the separatrix curve  $w_{CH}$  (50) for model C. As seen for model C in Figure 3, the parameter set  $w = 1.1, \tau = 4$  gives a dynamical evolution towards the stable fixed point given by (9,10). For the parameter set  $w = 1.3, \tau = 4$ , on the other hand, the system winds up in a stable limit cycle. This indicates that the transversal crossing across the separatrix  $w_{CH}$  corresponds to super-critical Hopf-bifurcations.

For the standard model and model B, both  $w = 1.1$  and  $w = 1.3$  are seen in Figure 2 to be below their respective separatrices  $w_{sH}$  and  $w_{BH}$ , and evolution toward a stable fixed point is seen in Figure 3. For model A, both  $w = 1.1$  and  $w = 1.3$  are seen in Figure 2 to be above its corresponding separatrix  $w_{AH}$ , and evolution toward stable limit cycles are seen in Figure 3.

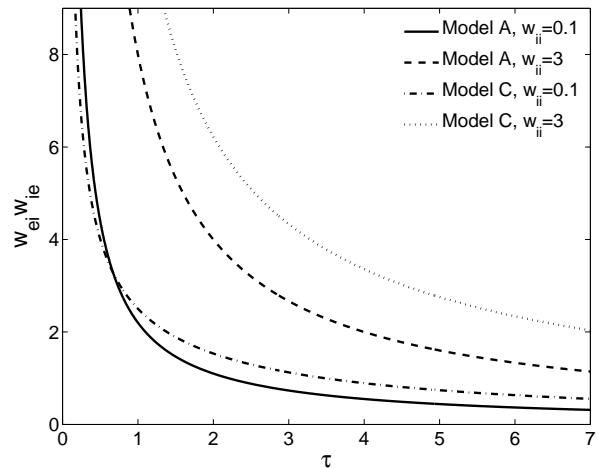


**Fig. 4** Curves separating parameter regimes predicting stable (below curves) and unstable equilibria (above curves) for example models A and C when the self-excitation is set to unity, i.e.,  $w_{ee} = 1$  for weak ( $w_{ii} = 0.1$ ) and strong ( $w_{ii} = 3$ ) self-inhibition. Solid line: model A,  $\eta_{AH}(\tau, w_{ii})$  (33),  $w_{ii} = 0.1$ . Dashed line: model A,  $\eta_{AH}(\tau, w_{ii})$  (33),  $w_{ii} = 3$ . Dash-dotted line: model C,  $\eta_{CH}(\tau, w_{ii})$  (51),  $w_{ii} = 0.1$ . Dotted line: model C,  $\eta_{CH}(\tau, w_{ii})$  (51),  $w_{ii} = 3$ .

Even though the equilibrium point in Fig. 3 corresponds to net synaptic drives on the oblique part of the piecewise-linear firing-rate function, parts of the depicted trajectories are outside this oblique part, i.e., on the constant parts, cf. Fig. 3. For example, in the panel for 'Model A,  $w=1.3$ ' the large limit-cycle trajectory both passes through regions where the net synaptic drive is smaller than the lower ( $\theta_e = \theta_i = -0.7$ ) and larger than the upper ( $\theta_e = \theta_i = 0.3$ ) cut-off points of the oblique part. Thus in this situation the predictions from the Hopf bifurcation analysis regarding the generation of a limit cycle appears to hold even though the vector field defining the system is not three-times continuously differentiable in the whole domain, as presupposed in Hopf's theorem.

*Fixed self-excitation.* While the standard model predicts stability in the whole parameter space when the self-excitation is set to unity, i.e.,  $w_{ee} = 1$ , this is not the case for the other models. For models A, B, and C the curves  $\eta_{AH}$  (33),  $\eta_{BH}$  (37), and  $\eta_{CH}$  (51) represent separatrices in the parameter space where points above the curves correspond to unstable equilibria and points below predict stable equilibria. This is illustrated in Figure 4 for models A and C for two particular choices of weights of self-inhibition  $w_{ii}$ . Note that model B is stable for the parameter values considered in this figure. Note also that the parameter regime that predicts stable equilibria in model A is contained in the stable parameter regime of model C, except when  $w_{ii}$  and  $\tau$  are sufficiently small, i.e.,  $0 < w_{ii} < 1 - 2\tau^2$ .

### 3 Discussion

The results in Figures 2 and 3 for the model with equal synaptic weights demonstrate that the choice of temporal coupling kernel can have a large effect on the stability properties of the (common) equilibrium point. A general observation is that instability is promoted by large inhibitory time constants  $\tau$ , a feature also observed for Turing-type instabilities in analogous rate models for a one-dimensional spatial continuum of neurons (Wyller et al. 2007).

In Figure 2 we also see that model A has the smallest regime of stability. This can be understood since the replacement of the exponentially decaying inhibitory temporal kernel with an  $\alpha$ -function (12) effectively corresponds to imposing a slower inhibitory dynamics. Conversely, model B is seen to have the largest stability regime. Here the slower excitatory dynamics modelled by an  $\alpha$ -function assures stability even for relatively large values of the time constant in the exponentially decaying inhibitory kernel. For model C where both temporal kernels are modelled as  $\alpha$ -functions we see that the stability separatrix lies between the corresponding separatrices of the standard model and model A, i.e., for a particular value of  $\tau$  it is more prone to stability than the standard model but less so than for model B.

In Figure 2 we also see that an increase of the synaptic weights promotes instability. Note that  $w_{mn}$  ( $m, n = e, i$ ) in this and the other figures correspond to a product of the synaptic weights in the original physiological model (4-5) multiplied by the steepness  $\beta_m$ ,  $m = e, i$ , of the firing-rate functions. Thus a steeper firing-rate function also promotes instability.

The situation  $w_{ee} = 1$  has particular significance. While unstable situations can always be found for the standard model when this self-excitation is larger than unity ( $w_{ee} > 1$ ),  $w_{ee} = 1$  or smaller assures stability. This makes intuitive sense: without an amplifying excitatory recurrent interaction, no instability is possible. However, for all of our alternative models, we found that instability is possible even with  $w_{ee} = 1$ . For these models we found unstable equilibrium points for sufficiently large cross-connection weights  $w_{ei}w_{ie}$ , i.e., for  $w_{ei}w_{ie} > \eta(\tau, w_{ii})$  where  $\eta(\tau, w_{ii})$  is given by (33) for model A, (37) for model B, and (51) for model C, respectively. Examples illustrating these instability regions of parameter space are shown in Figure 4 for models A and C. For the parameter-space window depicted here, model B was always found to provide stable equilibrium points.

A common feature of the separatrices  $\eta_{AH}(\tau, w_{ii})$  (33),  $\eta_{BH}(\tau, w_{ii})$  (37), and  $\eta_{CH}(\tau, w_{ii})$  (51) for the special case  $w_{ee} = 1$  is that they are monotonically increasing functions of the self-inhibition  $w_{ii}$ . Thus with a fixed time constant  $\tau$ , increased self-inhibition promotes stability of the equilibrium points. This is illustrated in Figure 4 for models A and C for specific parameter examples for  $w_{ee} = 1$ .

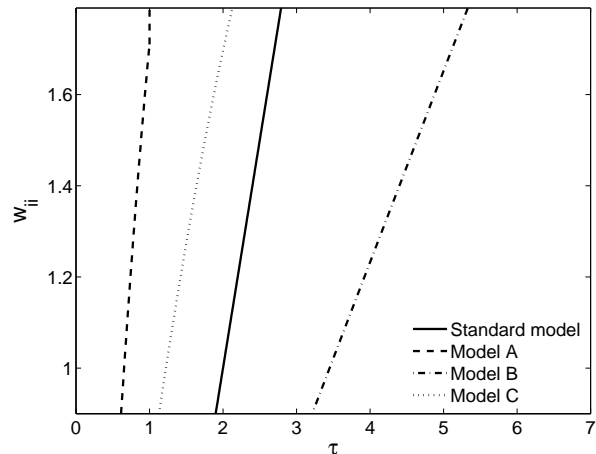


**Fig. 5** Illustration of parameter regimes producing stable (region left of curves) and unstable equilibria (region right of curves), respectively, for the four models considered. Model parameters:  $w_{ee} = 2$ ,  $w_{ei} = 1.9$ ,  $w_{ie} = 1.8$ ,  $\theta_e = \theta_i = -0.7$ . The depicted range of  $w_{ii}$  corresponds to a range for which the equilibrium points lie on the oblique parts of the firing-rate functions in (6).

One could suspect the situation  $w_{ee} = 1$  to be somewhat unrepresentative, however, since it corresponds to the border-line situation where the self-excitation is barely too weak to generate instabilities of the equilibrium points for the standard model. In Figure 5 we thus consider a different numerical example where the self-excitatory and cross-connection synaptic weights are well above unity, i.e.,  $w_{ee} = 2$ ,  $w_{ei} = 1.9$ , and  $w_{ie} = 1.8$ . For this choice of synaptic weights also the standard model exhibits regions of unstable equilibrium points, and we observe the same relative ordering between the models regarding their extent of stability regimes as in Figure 2 where all synaptic weights are equal: model B is most stable followed by the standard model, model C and model A. Except for this, the main qualitative features appears to be the same for the situation  $w_{ee} = 1$ : stability can be promoted by increasing the self-inhibition  $w_{ii}$  or by reducing the time constant  $\tau$ .

Presently we have investigated the stability properties of the various firing-rate models by means of mapping the Volterra systems to a set of coupled differential equations by means of the 'linear-chain-trick'. Alternatively, one could have obtained the same results by analyzing the Laplace-transformed versions of the linearized Volterra systems. An advantage with the mapping to a set of differential equations, however, is that such systems, being local in time, are more amenable to numerical explorations into the non-linear regime, as exemplified by Fig. 3.

With a one- or two-dimensional spatial continuum a richer variety of instabilities from the (homogeneous) background states is possible, for example stationary periodic patterns and spatiotemporally oscillations, see, e.g., Ermentrout and Cowan (1979a), Ermentrout and Cowan

(1979b), Ermentrout and Cowan (1980a), Ermentrout and Cowan (1980b), Hutt et al. (2003), Curtu and Ermentrout (2004), Hutt and Atay (2005), Atay and Hutt (2005), Atay and Hutt (2006), Wyller et al. (2007) and reviews by Ermentrout (1998), Bressloff (2005), and Coombes (2005). In the context of models in one or more spatial dimensions the present instability in the 'zero-dimensional' spatial model corresponds to an infinite-wavelength instability contrasting the finite-wavelength instabilities generating the periodic structures, see, e.g., Wyller et al. (2007). A natural extension of this work would thus be to see how the finite-wavelength instabilities in models in one spatial dimension are affected by other choices of temporal coupling kernels. Further, it would be of interest to go beyond linear stability analysis and investigate the generation of coherent structures such as traveling and standing waves and the stability of such structures (Ermentrout and Cowan 1980b; Curtu and Ermentrout 2004).

To conclude, we have found that for our synaptic-drive firing-rate models the choice of temporal coupling kernels can significantly affect the stability properties of the same equilibrium points. For most situations we find that a model with an  $\alpha$ -function replacing the standard exponentially decaying function in the inhibitory coupling kernel is most prone to instability while the opposite situation with an  $\alpha$ -function in the excitatory coupling kernel is least prone to instability. Further, stability is generally promoted by increasing the self-inhibition  $w_{ii}$  or shortening of the inhibitory time constant  $\tau$ .

## A Linear chain trick and Volterra equations

Any ODE system on the form

$$\tau_k x_k' = -x_k + f_k(\underline{x}), \quad k = 1, 2, \dots, N \quad (54)$$

can be converted to the system of Volterra equations

$$x_k(t) = \int_{-\infty}^t \frac{1}{\tau_k} e^{-(t-s)/\tau_k} f_k(\underline{x}(s)) ds, \quad k = 1, 2, \dots, N \quad (55)$$

by formal integration from  $-\infty$  to  $t$ . Here we consider the generalized version of (55), i.e.,

$$x_k = h_{n_k} * f_k(\underline{x}), \quad k = 1, 2, \dots, N \quad (56)$$

where  $h_{n_k} * f_k(\underline{x})$  is defined as the time convolution

$$[h_{n_k} * f_k(\underline{x})](t) \equiv \int_{-\infty}^t h_{n_k}(t-s) f_k(\underline{x}(s)) ds, \quad k = 1, 2, \dots, N \quad (57)$$

If  $\underline{f} = (f_1, f_2, \dots, f_N)$  is Lipschitz continuous, the component functions are bounded from above ( $|f_k| \leq M_k$  for some  $M_k > 0$ ), and  $h_{n_k}$  is bounded and has a countable set of jump discontinuities, the system (56) is globally well-posed (Cushing 1977).

We now consider this system when the integral kernel  $h_{n_k}(t)$  is given as

$$h_{n_k}(t) = \frac{1}{n_k!} \frac{1}{\tau_k} \left( \frac{t}{\tau_k} \right)^{n_k} e^{-t/\tau_k} \quad (58)$$

In this case the Volterra system (56) can be converted to an autonomous dynamical system:

$$\begin{aligned} \tau_k x_k' &= x_{k, n_k-1} - x_k \\ \tau_k x_{k, n_k-1}' &= x_{k, n_k-2} - x_{k, n_k-1} \\ &\vdots \\ \tau_k x_{k, 1}' &= x_{k, 0} - x_{k, 1} \\ \tau_k x_{k, 0}' &= f_k(\underline{x}) - x_{k, 0} \end{aligned} \quad (59)$$

In the process of deriving the  $n_k + 1$ -dimensional system (59) we have exploited the results.

$$\tau_k h_{n_k}'(t) = h_{n_k-1}(t) - h_{n_k}(t), \quad (60)$$

$$h_{n_k}(0) = \begin{cases} 0, & n_k = 1, 2, \dots, n_k - 1 \\ 1/\tau, & n_k = 0, \end{cases} \quad (61)$$

together with the differentiation rule

$$\frac{d}{dt} \left( \int_a^t F(t, s) ds \right) = F(t, t) + \int_a^t \frac{\partial}{\partial t} F(t, s) ds \quad (62)$$

where  $F$  and  $\frac{\partial F}{\partial t}$  are integrable and continuous, except for a set of measure zero, and differentiate (56) with respect to time. Finally, we have introduced the auxiliary variables

$$x_{k, n_k-j} = h_{n_k-j} * f_k(\underline{x}), \quad j = 1, 2, \dots, n_k \quad (63)$$

where  $h_{n_k-j}$  are given as

$$h_{n_k-j}(t) = \frac{1}{(n_k-j)!} \frac{1}{\tau_k} \left( \frac{t}{\tau_k} \right)^{n_k-j} e^{-t/\tau_k} \quad (64)$$

To conclude, we have thus proved that smooth solutions of the Volterra equation (56)-(58) obey a  $D$  dimensional autonomous dynamical system given by (59), where  $D$  is given by

$$D = \sum_{i=1}^N (n_i + 1) = N + \sum_{i=1}^N n_i \quad (65)$$

The technique employed in order to arrive at (59) is referred to as the linear chain trick. A detailed exposition of this can be found in Cushing (1977). In order to reproduce the standard firing-rate model in (15-16), we set  $N = 2$  and  $n_1 = n_2 = 0$ . Notice that any constant solution  $\underline{x}_0$  of (56)-(58) is an equilibrium of (59) i.e. it satisfies the fix point problem;

$$\underline{x} = \underline{F}(\underline{x}), \quad \underline{F} = (f_1, f_2, \dots, f_N) \quad (66)$$

Notice that  $\underline{x}_0$  also is an equilibrium solution for the system (54). Moreover, the stability issue of the constant solution of (56)-(58) can be resolved by means of standard stability theory for autonomous dynamical systems, i.e., in terms of the eigenvalues of the Jacobian  $\underline{J}$  of the vector-field defining (59), evaluated at  $\underline{x}_0$ .

Finally if the component functions  $x_k$ , ( $k = 1, 2, \dots, N$ ) satisfy a Volterra system on the form

$$x_k = h_{n_k} * f_k(\underline{x}) + p_{m_k} * g_k(\underline{x}), \quad (67)$$

we get global wellposedness if  $\underline{f} = f_1, f_2, \dots, f_N$  and  $\underline{g} = g_1, g_2, \dots, g_N$  are Lipschitz-continuous,  $f_k, g_k$  are bounded functions and the integral kernels  $h_{n_k}$  and  $p_{m_k}$  are bounded with

a countable set of jump discontinuities. Assume that the temporal kernels  $h_{n_k}$  and  $p_{m_k}$  are modelled by

$$h_{n_k}(t) = \frac{1}{n_k!} \frac{1}{\tau_{fk}} \left( \frac{t}{\tau_{fk}} \right)^{n_k} e^{-t/\tau_{fk}} \quad (68)$$

$$p_{m_k}(t) = \frac{1}{m_k!} \frac{1}{\tau_{gk}} \left( \frac{t}{\tau_{gk}} \right)^{m_k} e^{-t/\tau_{gk}} \quad (69)$$

and introduce the auxiliary variables  $y_k = h_{n_k} * f_k(\underline{x})$ ,  $z_k = p_{m_k} * g_k(\underline{x}(t))$ , then by employing the same procedure as above for each of the variables  $y_k$  and  $z_k$  and derives an autonomous dynamical system. The dimension of the resulting system is given as

$$D = \sum_{k=1}^N (n_k + m_k) + 2N \quad (70)$$

Notice that the coupling between the  $y_k$  and  $z_k$  variables is given by the constraint  $x_k = y_k + z_k$ , ( $k = 1, 2, \dots, N$ ) The constant solutions of (67) corresponds to the equilibrium of the dynamical system.

## B Routh-Hurwitz criterion and Hopf-bifurcations

### B.1 Routh-Hurwitz criterion

The stability of an equilibrium point of an autonomous dynamical system is determined by the eigenvalues of the Jacobian evaluated at that equilibrium point. An equilibrium is asymptotically stable if all the eigenvalues  $\lambda_i$  ( $i = 1, 2, \dots, N$ ) possess the property  $Re\lambda_i < 0$ . The Routh-Hurwitz criterion yields a necessary and sufficient condition for having asymptotic stability (Murray 1993). It can be formulated as follows: Let  $P_N(\lambda)$  be the polynomial  $P(\lambda) = \lambda^N + a_1\lambda^{N-1} + \dots + a_{N-1}\lambda + a_N$  and introduce the matrices

$$\begin{aligned} \mathbf{D}_1 &= a_1 \\ \mathbf{D}_2 &= \begin{bmatrix} a_1 & a_3 \\ 1 & a_2 \end{bmatrix} \\ \mathbf{D}_3 &= \begin{bmatrix} a_1 & a_3 & a_5 \\ 1 & a_2 & a_4 \\ 0 & a_1 & a_3 \end{bmatrix} \\ \mathbf{D}_k &= \begin{bmatrix} a_1 & a_3 & \dots & \dots \\ 1 & a_2 & a_4 & \dots \\ 0 & a_1 & a_3 & \dots \\ 0 & 1 & a_2 & \dots \\ \dots & \dots & \dots & \dots \\ 0 & 0 & \dots & a_k \end{bmatrix} \quad k = 1, 2, \dots, N. \end{aligned} \quad (71)$$

Then the following equivalence holds true:

$$\begin{aligned} |\mathbf{D}_k| \equiv \det[\mathbf{D}_k] > 0, \quad k = 1, 2, \dots, N \wedge a_N \neq 0 \\ \iff Re(\lambda_i) < 0, \quad (i = 1, 2, \dots, N) \end{aligned} \quad (72)$$

where  $\lambda_i$ , ( $i = 1, 2, \dots, N$ ) denote the zeros of  $P_N(\lambda)$ ;  $P_N(\lambda_i) = 0$ .

### B.2 Hopf bifurcation and breakdown of the Routh-Hurwitz criterion

*Two-dimensional systems.* For a two-dimensional autonomous dynamical system the characteristic polynomial  $P_2(\lambda)$  is given as

$$P_2(\lambda) = \lambda^2 - tr[\mathbf{J}]\lambda + det[\mathbf{J}] \quad (73)$$

In this case the Routh-Hurwitz determinants  $|\mathbf{D}_1|$ ,  $|\mathbf{D}_2|$  are given by the trace and the determinant to the corresponding Jacobian.

$$|\mathbf{D}_1| = -tr[\mathbf{J}] \quad (74)$$

$$|\mathbf{D}_2| = det[\mathbf{J}] \quad (75)$$

According to the fundamental theorem of algebra, the quadratic polynomial  $P_2$  has two zeros, counted with multiplicity. Since by assumption the trace and the determinant of  $\mathbf{J}$  are real, complex zeros appear in complex conjugate pairs. Now let  $\lambda = \mu \pm i\gamma$ . denote the pair of complex conjugate zeros of  $P_2$ . Then  $P_2$  can be factorized as

$$P_2(\lambda) = (\lambda + (\mu + i\gamma))(\lambda + (\mu - i\gamma)) \quad (76)$$

Assume the zeros are purely imaginary, i.e.,  $\lambda = \pm i\gamma$ . Then  $P_2$  is given as

$$P_2(\lambda) = \lambda^2 + \gamma^2 \quad (77)$$

We compute the trace  $tr[\mathbf{J}]$  and the determinant  $det[\mathbf{J}]$  in this case and find that

$$\begin{aligned} tr[\mathbf{J}] &= 0 \\ det[\mathbf{J}] &= \gamma^2 \end{aligned} \quad (78)$$

Thus we conclude that purely imaginary eigenvalues in the characteristic polynomial  $P_2$  implies  $tr[\mathbf{J}] = 0$ . Let us now show that the assumptions  $tr[\mathbf{J}] = 0$  and  $det[\mathbf{J}] > 0$  implies that  $P_2$  has two purely imaginary eigenvalues. We proceed as follows: Introduce the positive real number  $\gamma$  defined as

$$\gamma = \sqrt{det[\mathbf{J}]} \quad (79)$$

The assumption  $tr[\mathbf{J}] = 0$  implies that the characteristic polynomial  $P_2$  can be written as

$$P_2(\lambda) = \lambda^2 + det[\mathbf{J}] \quad (80)$$

One then easily deduces that

$$P_2(\pm i\gamma) = 0 \quad (81)$$

by simple computation. Finally let us now relate the theory of generic Hopf bifurcation to the breakdown of the positivity of  $tr[\mathbf{J}]$ . Let the autonomous dynamical system under consideration be a two-dimensional system which we for convenience denote as  $\underline{x}' = \underline{G}(\underline{x}, \alpha)$ , where the vector field  $\underline{G}$  is locally at least three times continuously differentiable in an open, simply connected set about the equilibrium point (Perko 2000). Here  $\underline{x}$  is the phase-space variable, while  $\alpha$  denotes the control variable. In this case any equilibrium traces out a curve in the phase space. Moreover, the coefficients of the characteristic polynomial  $P_2$  depends on  $\alpha$ ;  $tr[\mathbf{J}] = tr[\mathbf{J}](\alpha)$  and  $det[\mathbf{J}] = det[\mathbf{J}](\alpha)$ . We assume that there exists a critical  $\alpha$ -value denoted by  $\alpha_c$  such that

- (i)  $\underline{G}(\underline{x}_0(\alpha_c), \alpha_c) = 0$ .
- (ii) The Jacobian  $\frac{\partial \underline{G}}{\partial \underline{x}}(\underline{x}_0(\alpha_c), \alpha_c)$  possesses purely imaginary eigenvalues:  $\lambda(\alpha_c) = \pm i\gamma_c$ .
- (iii)  $\lambda(\alpha)$  is an analytic function of  $\alpha$  for which the transversality conditions  $\frac{d}{d\alpha} Re[\lambda(\alpha)]|_{\alpha=\alpha_c} \neq 0$  hold.

Hopf's theorem implies that a Hopf bifurcation will take place at  $\alpha = \alpha_c$ , i.e., a limit cycle will be excited as we pass this critical value. The Routh-Hurwitz formalism for  $P_2$  enables us to translate the condition (ii) for having purely imaginary eigenvalues into a condition on the trace  $tr[\mathbf{J}]$

$$tr[\mathbf{J}](\alpha = \alpha_c) = 0, \quad \text{and} \quad det[\mathbf{J}](\alpha = \alpha_c) > 0 \quad (82)$$

Moreover, notice that we have the following equivalence:

$$\frac{d}{d\alpha} \operatorname{Re}[\lambda(\alpha)]|_{\alpha=\alpha_c} \neq 0 \iff \frac{d}{d\alpha} \operatorname{tr}[\mathbf{J}]|_{\alpha=\alpha_c} \neq 0 \quad (83)$$

This can be shown as follows: Assume  $\frac{\partial P_2}{\partial \lambda}(\pm i\gamma_c, \alpha_c) \neq 0$ . Then, by the implicit function theorem,  $\lambda$  is an analytical function of  $\alpha$ , and

$$\begin{aligned} \frac{d\lambda}{d\alpha}\Big|_{\alpha=\alpha_c} &= -\left[\frac{\partial P_2}{\partial \alpha} / \frac{\partial P_2}{\partial \lambda}\right]\Big|_{(\lambda=\pm i\gamma_c, \alpha=\alpha_c)} \\ &= -\frac{-\operatorname{tr}[\mathbf{J}']\lambda + \det[\mathbf{J}']}{2\lambda + \operatorname{tr}[\mathbf{J}']}\Big|_{(\lambda=\pm i\gamma_c, \alpha=\alpha_c)} \end{aligned} \quad (84)$$

Simple computations reveal that

$$\operatorname{Re}\left[-\frac{-\operatorname{tr}[\mathbf{J}']\lambda + \det[\mathbf{J}']}{2\lambda + \operatorname{tr}[\mathbf{J}']}\right]\Big|_{(\lambda=\pm i\gamma_c, \alpha=\alpha_c)} = 0 \quad (85)$$

if and only if

$$2\operatorname{tr}[\mathbf{J}'](\alpha_c)\det[\mathbf{J}](\alpha_c) = 0 \quad (86)$$

Now, by assumption  $\det[\mathbf{J}] > 0$ . Hence we arrive at the result (83).

*Three-dimensional systems.* For a three-dimensional autonomous dynamical system the characteristic polynomial  $P_3(\lambda)$  of the Jacobian evaluated at the equilibrium point is a cubic polynomial:

$$P_3(\lambda) = \lambda^3 + a_1\lambda^2 + a_2\lambda + a_3 \quad (87)$$

In this case the matrixes  $\mathbf{D}_1$ ,  $\mathbf{D}_2$ , and  $\mathbf{D}_3$  are given as

$$\begin{aligned} \mathbf{D}_1 &= a_1 \\ \mathbf{D}_2 &= \begin{bmatrix} a_1 & a_3 \\ 1 & a_2 \end{bmatrix} \\ \mathbf{D}_3 &= \begin{bmatrix} a_1 & a_3 & 0 \\ 1 & a_2 & 0 \\ 0 & a_1 & a_3 \end{bmatrix} \end{aligned} \quad (88)$$

and the determinants  $|\mathbf{D}_1|$ ,  $|\mathbf{D}_2|$  and  $|\mathbf{D}_3|$  can hence be computed as

$$\begin{aligned} |\mathbf{D}_1| &= a_1 \\ |\mathbf{D}_2| &= a_1 a_2 - a_3 \\ |\mathbf{D}_3| &= a_3 |\mathbf{D}_2| \end{aligned} \quad (89)$$

According to the fundamental theorem of algebra, the cubic polynomial  $P_3$  has three zeros, counted with multiplicity. Since by assumption the coefficients of  $P_3$  are real, complex zeros appear in complex conjugate pairs. Now let  $\lambda = \mu \pm i\gamma$  denote the pair of complex conjugate zeros of  $P_3$ . Then  $P_3$  can be factorized as

$$P_3(\lambda) = (\lambda + (\mu + i\gamma))(\lambda + (\mu - i\gamma))(\lambda + x) \quad (90)$$

Assume the zeros are purely imaginary, i.e.,  $\lambda = \pm i\gamma$ . Then  $P_3$  is given as

$$P_3(\lambda) = \lambda^3 + x\lambda^2 + \gamma^2\lambda + x\gamma^2 \quad (91)$$

We compute the determinants  $|\mathbf{D}_1|$ ,  $|\mathbf{D}_2|$ , and  $|\mathbf{D}_3|$  in this case and find that

$$\begin{aligned} |\mathbf{D}_1| &= x \\ |\mathbf{D}_2| &= x\gamma^2 - x\gamma^2 = 0 \\ |\mathbf{D}_3| &= x\gamma^2 |\mathbf{D}_2| = 0 \end{aligned} \quad (92)$$

Thus we conclude that purely imaginary eigenvalues in the characteristic polynomial  $P_3$  implies  $|\mathbf{D}_2| = 0$ . Let us now show that the assumptions  $|\mathbf{D}_2| = 0$  and  $\operatorname{sgn}[a_3] = \operatorname{sgn}[a_1]$  implies that  $P_3$  has two purely imaginary eigenvalues. We proceed as follows: Introduce the positive real number  $\gamma$  defined as

$$\gamma = \sqrt{\frac{a_3}{a_1}} \quad (93)$$

The assumption  $|\mathbf{D}_2| = 0$  implies that the characteristic polynomial  $P_3$  can be written as

$$P_3(\lambda) = \lambda^3 + a_1\lambda^2 + \frac{a_3}{a_1}\lambda + a_3 \quad (94)$$

One then easily deduces that

$$P_3(\pm i\gamma) = 0 \quad (95)$$

by simple computation. Finally let us now relate the theory of generic Hopf bifurcation to the breakdown of the positivity of  $|\mathbf{D}_2|$  in the Routh-Hurwitz criterion. Let the autonomous dynamical system under consideration be the three-dimensional system  $\dot{\mathbf{x}} = \mathcal{G}(\mathbf{x}, \alpha)$ , where the vector field  $\mathcal{G}$  is locally at least three times continuously differentiable in an open, simply connected set about the equilibrium point (Perko 2000). Here  $\mathbf{x}$  is the phase-space variable, while  $\alpha$  denotes the control variable. In this case any equilibrium traces out a curve in the phase space. Moreover, the coefficients of the characteristic polynomial  $P_3$  depends on  $\alpha$ ;  $a_i = a_i(\alpha)$ , ( $i = 1, 2, 3$ ). We assume that there exists a critical  $\alpha$ -value denoted by  $\alpha_c$  such that

- (i)  $\mathcal{G}(\mathbf{x}_0(\alpha_c), \alpha_c) = 0$ .
- (ii) The Jacobian  $\frac{\partial \mathcal{G}}{\partial \mathbf{x}}(\mathbf{x}_0(\alpha_c), \alpha_c)$  possesses purely imaginary eigenvalues:  $\lambda(\alpha_c) = \pm i\gamma_c$ .
- (iii)  $\lambda(\alpha)$  is an analytic function of  $\alpha$  for which the transversality conditions  $\frac{d}{d\alpha} \operatorname{Re}[\lambda(\alpha)]|_{\alpha=\alpha_c} \neq 0$  hold.
- (iv) The remaining eigenvalue is nonzero

Hopf's theorem implies that a Hopf bifurcation will take place at  $\alpha = \alpha_c$ , i.e., a limit cycle will be excited as we pass this critical value. The Routh-Hurwitz formalism for  $P_3$  enables us to translate the condition (ii) for having purely imaginary eigenvalues into a condition on the sub-determinant  $|\mathbf{D}_2|$ :

$$|\mathbf{D}_2|(\alpha = \alpha_c) = 0, \quad \text{and} \quad \operatorname{sgn}[a_3(\alpha_c)] = \operatorname{sgn}[a_1(\alpha_c)] \quad (96)$$

The condition (iv) is fulfilled if and only if the coefficient  $a_3$  is nonzero. Moreover, notice that we have the following equivalence:

$$\frac{d}{d\alpha} \operatorname{Re}[\lambda(\alpha)]|_{\alpha=\alpha_c} \neq 0 \iff \frac{d}{d\alpha} |\mathbf{D}_2|_{\alpha=\alpha_c} \neq 0 \quad (97)$$

We prove this by proceeding in a way analogous to Liao et al. (2003): Assume  $\frac{\partial P_3}{\partial \lambda}(\pm i\gamma_c, \alpha_c) \neq 0$ . Then, by the implicit function theorem,  $\lambda$  is an analytical function of  $\alpha$ , and

$$\begin{aligned} \frac{d\lambda}{d\alpha}\Big|_{\alpha=\alpha_c} &= -\left[\frac{\partial P_3}{\partial \alpha} / \frac{\partial P_3}{\partial \lambda}\right]\Big|_{(\lambda=\pm i\gamma_c, \alpha=\alpha_c)} \\ &= -\frac{a_1'\lambda^2 + a_2'\lambda + a_3'}{3\lambda^2 + 2a_1\lambda + a_2}\Big|_{(\lambda=\pm i\gamma_c, \alpha=\alpha_c)} \end{aligned} \quad (98)$$

Simple computations reveal that

$$\operatorname{Re}\left[-\frac{a_1'\lambda^2 + a_2'\lambda + a_3'}{3\lambda^2 + 2a_1\lambda + a_2}\right]\Big|_{(\lambda=\pm i\gamma_c, \alpha=\alpha_c)} = 0 \quad (99)$$

if and only if

$$n(\alpha_c) = 0 \quad (100)$$

where

$$n(\alpha_c) = -a_1' \left( \frac{a_3}{a_1} \right)^2 - a_2' a_3 + a_3' \left( \frac{a_3}{a_1} \right) \quad (101)$$

On the other hand, by differentiating  $|\mathbf{D}_2|$  with respect to  $\alpha$ , we find that

$$\frac{d|\mathbf{D}_2|}{d\alpha} \Big|_{\alpha=\alpha_c} = n(\alpha_c) \left( -\frac{a_1}{a_3} \right) \quad (102)$$

Hence we arrive at the result (97).

*Four-dimensional systems.* For a four-dimensional autonomous dynamical system the characteristic polynomial  $P_4(\lambda)$  of the Jacobian evaluated at the equilibrium is a quartic polynomial:

$$P_4(\lambda) = \lambda^4 + a_1\lambda^3 + a_2\lambda^2 + a_3\lambda + a_4 \quad (103)$$

In this case the matrixes  $\mathbf{D}_1$ ,  $\mathbf{D}_2$ ,  $\mathbf{D}_3$  and  $\mathbf{D}_4$  are given as

$$\begin{aligned} \mathbf{D}_1 &= a_1 \\ \mathbf{D}_2 &= \begin{bmatrix} a_1 & a_3 \\ 1 & a_2 \end{bmatrix} \\ \mathbf{D}_3 &= \begin{bmatrix} a_1 & a_3 & 0 \\ 1 & a_2 & a_4 \\ 0 & a_1 & a_3 \end{bmatrix} \\ \mathbf{D}_4 &= \begin{bmatrix} a_1 & a_3 & 0 & 0 \\ 1 & a_2 & a_4 & 0 \\ 0 & a_1 & a_3 & 0 \\ 0 & 1 & a_2 & a_4 \end{bmatrix} \end{aligned} \quad (104)$$

and the determinants  $|\mathbf{D}_1|$ ,  $|\mathbf{D}_2|$ ,  $|\mathbf{D}_3|$  and  $|\mathbf{D}_4|$  can hence be computed as

$$\begin{aligned} |\mathbf{D}_1| &= a_1 \\ |\mathbf{D}_2| &= a_1 a_2 - a_3 \\ |\mathbf{D}_3| &= a_1 a_2 a_3 - a_1^2 a_4 - a_3^2 \\ |\mathbf{D}_4| &= a_4 |\mathbf{D}_3| \end{aligned} \quad (105)$$

According to the fundamental theorem of algebra, the quartic polynomial  $P_4$  has four zeros, counted with multiplicity. Since by assumption the coefficients of  $P_4$  are real, complex zeros appear in complex conjugate pairs. Now let  $\lambda = \mu \pm i\gamma$ , denote the pair of complex conjugate zeros of  $P_4$ . Then  $P_4$  can be factorized as

$$P_4(\lambda) = (\lambda + (\mu + i\gamma))(\lambda + (\mu - i\gamma))(\lambda^2 + a\lambda + b). \quad (106)$$

Assume the zeros are purely imaginary, i.e.,  $\lambda = \pm i\gamma$ . Then  $P_4$  is given as

$$P_4(\lambda) = \lambda^4 + a\lambda^3 + (b + \gamma^2)\lambda^2 + a\gamma^2\lambda + b\gamma^2 \quad (107)$$

We compute the determinants  $|\mathbf{D}_1|$ ,  $|\mathbf{D}_2|$ ,  $|\mathbf{D}_3|$  and  $|\mathbf{D}_4|$  in this case and find that

$$\begin{aligned} |\mathbf{D}_1| &= a \\ |\mathbf{D}_2| &= ab \\ |\mathbf{D}_3| &= a((b + \gamma^2)a\gamma^2 - ab\gamma^2) - a\gamma^2 a\gamma^2 = 0 \\ |\mathbf{D}_4| &= b\gamma^2 |\mathbf{D}_3| = 0 \end{aligned} \quad (108)$$

Thus we conclude that purely imaginary eigenvalues in the characteristic polynomial  $P_4$  implies  $|\mathbf{D}_3| = 0$ . Let us now show that the assumptions  $|\mathbf{D}_3| = 0$  and  $\text{sgn}[a_3] = \text{sgn}[a_1]$  imply that  $P_4$  has two purely imaginary eigenvalues (Liao et

al. 2003). We proceed as follows: Introduce the positive real number  $\gamma$  defined as

$$\gamma = \sqrt{\frac{a_3}{a_1}} \quad (109)$$

The assumption  $|\mathbf{D}_3| = 0$  implies that the characteristic polynomial  $P_4$  can be written as

$$P_4(\lambda) = \lambda^4 + a_1\lambda^3 + a_2\lambda^2 + a_3\lambda + \frac{(a_1 a_2 - a_3) a_3}{a_1^2}. \quad (110)$$

One then easily deduces that

$$P_4(\pm i\gamma) = 0 \quad (111)$$

by simple computation. Finally let us now relate the theory of generic Hopf bifurcation to the breakdown of the positivity of  $|\mathbf{D}_3|$  in the Routh-Hurwitz criterion. Let the four-dimensional system be given as  $\dot{\underline{x}} = \underline{G}(\underline{x}, \alpha)$ , where the vector field  $\underline{G}$  is locally at least three times continuously differentiable in an open, simply connected set about the equilibrium point (Perko 2000). Here  $\underline{x}$  is the phase-space variable, while  $\alpha$  denotes the control variable. In this case any equilibrium traces out a curve in the phase space. Moreover, the coefficients of the characteristic polynomial  $P_4$  depends on  $\alpha$ ;  $a_i = a_i(\alpha)$ , ( $i = 1, 2, 3, 4$ ). We assume that there exists a critical  $\alpha$ -value denoted by  $\alpha_c$  such that

- (i)  $\underline{G}(\underline{x}_0(\alpha_c), \alpha_c) = 0$ .
- (ii) The Jacobian  $\frac{\partial \underline{G}}{\partial \underline{x}}(\underline{x}_0(\alpha_c), \alpha_c)$  possesses purely imaginary eigenvalues:  $\lambda(\alpha_c) = \pm i\gamma_c$ .
- (iii)  $\lambda(\alpha)$  is an analytic function of  $\alpha$  for which the transversality conditions  $\frac{d}{d\alpha} \text{Re}[\lambda(\alpha)]|_{\alpha=\alpha_c} \neq 0$  hold.
- (iv) The two remaining eigenvalues have nonzero real parts.

Hopf's theorem implies that a Hopf bifurcation will take place at  $\alpha = \alpha_c$ , i.e., a limit cycle will be excited as we pass this critical value. The Routh-Hurwitz formalism for  $P_4$  enables us to translate the condition (ii) for having purely imaginary eigenvalues into a condition on the sub-determinant  $|\mathbf{D}_3|$ :

$$|\mathbf{D}_3|(\alpha = \alpha_c) = 0, \quad \text{and} \quad \text{sgn}[a_3(\alpha_c)] = \text{sgn}[a_1(\alpha_c)] \quad (112)$$

Notice that we must have  $a_4(\alpha_c) > 0$ ,  $a_3(\alpha_c) \neq 0$  and  $a_1(\alpha_c) \neq 0$  to get the condition (iv) fulfilled. Moreover, notice that we have the following equivalence:

$$\frac{d}{d\alpha} \text{Re}[\lambda(\alpha)]|_{\alpha=\alpha_c} \neq 0 \iff \frac{d}{d\alpha} |\mathbf{D}_3|_{\alpha=\alpha_c} \neq 0 \quad (113)$$

Again we proceed in a way analogous to Liao et al. (2003): Assume  $\frac{\partial P_4}{\partial \lambda}(\pm i\gamma_c, \alpha_c) \neq 0$ . Then, by the implicit function theorem,  $\lambda$  is an analytical function of  $\alpha$ , and

$$\begin{aligned} \frac{d\lambda}{d\alpha} \Big|_{\alpha=\alpha_c} &= - \left[ \frac{\partial P_4}{\partial \alpha} / \frac{\partial P_4}{\partial \lambda} \right] \Big|_{(\lambda=\pm i\gamma_c, \alpha=\alpha_c)} \\ &= - \frac{a_1' \lambda^3 + a_2' \lambda^2 + a_3' \lambda + a_4'}{4\lambda^3 + 3a_1 \lambda^2 + 2a_2 \lambda + a_3} \Big|_{(\lambda=\pm i\gamma_c, \alpha=\alpha_c)} \end{aligned} \quad (114)$$

Simple computations reveal that

$$\text{Re} \left[ - \frac{a_1' \lambda^3 + a_2' \lambda^2 + a_3' \lambda + a_4'}{4\lambda^3 + 3a_1 \lambda^2 + 2a_2 \lambda + a_3} \right] \Big|_{(\lambda=\pm i\gamma_c, \alpha=\alpha_c)} = 0 \quad (115)$$

if and only if

$$n(\alpha_c) = 0 \quad (116)$$

where

$$n(\alpha_c) = 2a_3 \left( \frac{a_3' a_2}{a_1} - \frac{2a_3' a_3}{a_1^2} - \frac{a_1' a_2 a_3}{a_1^2} + \frac{2a_1' a_3^2}{a_1^3} + \frac{a_2' a_3}{a_1} - a_4' \right) \quad (117)$$

On the other hand, by differentiating  $|\mathbf{D}_3|$  with respect to  $\alpha$ , we find that.

$$\frac{d|\mathbf{D}_3|}{d\alpha} \Big|_{\alpha=\alpha_c} = n(\alpha_c) \frac{a_1^2}{a_3} \quad (118)$$

Hence we arrive at the result (113).

*General finite dimensional systems.* The theory elaborated for 2, 3 and 4 dimensional systems can be generalized to  $N$ -dimensional systems. The autonomous dynamical system for an  $N$ -dimensional system is for convenience denoted  $\underline{x}' = \underline{G}(\underline{x}, \alpha)$  where  $\underline{x}$  is the phase-space variable, and  $\alpha$  denotes the control variable. The vector field  $\underline{G}$  is assumed to be at least three times continuously differentiable in an open, simple connected set about the equilibrium. In this case any equilibrium traces out a curve in the phase space. Moreover, the coefficients of the characteristic polynomial  $P_N$  depends on  $\alpha$ ;  $a_n = a_n(\alpha)$ , ( $n = 1, 2, 3, \dots, N$ ). We assume that there exists a critical  $\alpha$ -value denoted by  $\alpha_c$  such that

- (i)  $\underline{G}(\underline{x}_0(\alpha_c), \alpha_c) = 0$ .
- (ii) The Jacobian  $\frac{\partial \underline{G}}{\partial \underline{x}}(\underline{x}_0(\alpha_c), \alpha_c)$  possesses purely imaginary eigenvalues:  $\lambda(\alpha_c) = \pm i\gamma_c$ .
- (iii)  $\lambda(\alpha)$  is an analytic function of  $\alpha$  for which the transversality conditions  $\frac{d}{d\alpha} \operatorname{Re}[\lambda(\alpha)] \Big|_{\alpha=\alpha_c} \neq 0$  hold.
- (iv) The remaining eigenvalues have nonzero real parts.

Hopf's theorem implies that a Hopf-bifurcation will take place at  $\alpha = \alpha_c$ , i.e., a limit cycle will be excited as we pass this critical value. Let  $\mathbf{D}_k(\alpha_c)$  denote the  $k$  Routh-Hurwitz determinant. Then the following criteria guarantee that the conditions (ii) and (iii) are fulfilled (Jing and Ling 1993; Shen and Jing 1993):  $\mathbf{D}_{N-1}(\alpha_c) = 0$ ,  $\mathbf{D}_{N-2}(\alpha_c) \neq 0$ ,  $\mathbf{D}_{N-3}(\alpha_c) \neq 0$ ,  $a_n(\alpha_c) > 0$  for  $n = 1, 2, \dots, N$  and  $\frac{d}{d\alpha} |\mathbf{D}_{N-1}|_{\alpha=\alpha_c} \neq 0$ .

**Acknowledgements** The authors will like to thank A. Ponosov (Norwegian University of Life Sciences) for many fruitful and stimulating discussions during the preparation of this paper. We will also like to thank the reviewers for constructive comments and suggestions.

## References

- Amari S (1977) Dynamics of pattern formation in lateral-inhibition type neural fields. *Biol Cybernet* 27:77–87
- Atay FM, Hutt A (2005) Stability and bifurcations in neural fields with finite propagation speed and general connectivity *SIAM J Appl Math* 65:644–666
- Atay FM, Hutt A (2006) Neural fields with distributed transmission speeds and long-range feedback delays *SIAM J Appl Dyn Syst* 5:670–698
- Bressloff P (2005) Pattern formation in visual cortex. In: Chow C, Gutkin B, Hansel D, Meunier C, Dalibard J (eds) *Methods and Models in Neurophysics: Lecture Notes of the Les Houches Summer School 2003*, Elsevier, Amsterdam, pp. 477–574.
- Coombes S (2005) Waves, bumps, and patterns in neural field theories *Biol Cybern* 93:91–108
- Curtu R, Ermentrout B (2004) Pattern formation in a network of excitatory and inhibitory cells with adaptation *SIAM J Appl Dyn Syst* 3:191–231

Cushing JM (1977) *Integrodifferential Equations and Delay Models in Population Dynamics*, Lecture Notes in Biomathematics. Springer, New York.

Dayan P and Abbott LW (2001) *Theoretical Neuroscience*, MIT Press, Cambridge, Massachusetts.

Ermentrout GB, Cowan J (1979a) Temporal oscillations in neuronal nets *J Math Biol* 7:265–280

Ermentrout GB, Cowan J (1979b) A mathematical theory of visual hallucination patterns *Biol Cybern* 34:137–150

Ermentrout GB, Cowan J (1980a) Large scale spatially organized activity in neural nets *SIAM J Appl Math* 38:1–21

Ermentrout GB, Cowan J (1980b) Secondary bifurcations in neuronal nets *SIAM J Appl Math* 39:323–340

Ermentrout B (1998) Neural networks as spatio-temporal pattern-forming systems *Rep Prog Phys* 61:353–430

Hutt A, Bestehorn M, Wennekers T (2003) Pattern formation in intracortical neural fields *Netw Comp Neur Syst* 14:351–368

Hutt A, Atay FM (2005) Analysis of nonlocal neural fields for both general and gamma-distributed connectivities *Physica D* 203:30–54

Jing ZJ, Lin Z (1993) Qualitative analysis for a mathematical model for AIDS. *Acta Mathematicae Appl Sinica* 9:302–316

Koch C (1999) *Biophysics of Computation*, Oxford University Press, New York.

Laing CR and Longtin A (2003) Dynamics of deterministic and stochastic paired excitatory-inhibitory delayed feedback. *Neural Comput* 15:2779–2822

Liao X, Wong K, Wu X (2003) Stability of bifurcating periodic solutions for van der Pol equation with continuous distributed delay. *Applied Mathematics and Computation* 146:313–334.

Linz P (1985) *Analytical and Numerical Methods for Volterra Equations*, SIAM, Philadelphia, PA:

Murray JD (1993) *Mathematical Biology*, Second Edition, Wiley-Interscience, Hoboken, NJ.

Perko L (2000) *Differential Equations and Dynamical Systems*, 3rd ed., in: *Texts in Applied Mathematics*, vol. 7, Springer-Verlag, New York, NY.

Pinto DJ, Brumberg JC, Simons DJ, Ermentrout GB (1996) A quantitative population model of whisker barrels: re-examining the Wilson-Cowan equations. *J Comput Neurosci* 3:247–264

Tateno T, Harsch A, Robinson HPC (2004) Threshold firing frequency-current relationships of neurons in rat somatosensory cortex: type 1 and type 2 dynamics. *J Neurophysiol* 92:2283–2294

Tsodyks MV, Skaggs WE, Sejnowski TJ, McNaughton BL (1997) Paradoxical effects of external modulation of interneurons. *J Neurosci* 17:4382–4388

Wilson HR, Cowan JD (1973) A mathematical theory of the functional dynamics of cortical and thalamic nervous tissue. *Kybernetik* 13:55–80

Shen J and Jing ZJ (1993) A new detecting method for conditions of existence of Hopf bifurcation. *Acta Math Appl Sinica* 11:79–93

Vogels TP, Rajan K, Abbott LF (2005) Neural network dynamics *Ann Rev Neurosci* 28:357–376

Wyller J, Blomquist P, Einevoll GT (2007) Turing instability and pattern formation in a two-population neuronal network model. *Physica D* 225:75–93